

1 Effect Of Temperature On The Dynamic 2 Response Of Adhesively Mounted 3 Accelerometers

4 **Andrea Spaggiari¹ and Marco Cocconcelli²**

5 ¹**Department of Engineering Sciences and Methods, University of Modena and Reggio
6 Emilia, Italy, E-mail: andrea.spaggiari@unimore.it**

7 ²**Department of Engineering Sciences and Methods, University of Modena and Reggio
8 Emilia, Italy, E-mail: marco.cocconcelli@unimore.it**

9 **ABSTRACT**

10 This paper focuses on the effect of temperature on the frequency response function (FRF) of three
11 different structural adhesives; namely a two component methylmethacrylate (HBM X60), a modified
12 silane (Terostat 939) and a cyanoacrylate (Loctite 454). The structural adhesives are commonly used in
13 vibration analysis to mount accelerometers on structures or machines. The stiffness of the adhesive can
14 influence the response function on large frequency band, affecting the proportional excitation between
15 the structure and the accelerometer. In the “system structure + adhesive + accelerometer”, the adhesive
16 may acts like a filter between the source and the sink of vibrations. A variation of the dynamic response
17 of the filter could lead to an erroneous analysis. The authors already investigated the relation between
18 the frequency response function and operating conditions of the test. This paper expands the research
19 by considering the temperature effect in order to depict a complete picture of the adhesive behavior
20 on dynamic response of an accelerometer. A design of experiments (DOE) approach was used to test
21 two bonded aluminium bases at different levels of temperature and frequency of the external sinusoidal
22 excitation, supplied by an electromagnetic shaker. The results clearly demonstrate that the adhesive is
23 not able to change the system response, therefore the signal transmission is good in the entire range of
24 temperature regardless the adhesive chosen.

25 **Keywords:** Temperature, Mechanical properties of adhesives, Accelerometers mounting, Vibration
26 transmissivity, Experimental testing

27 **1 INTRODUCTION**

28 Accelerometers are widely used in reliability and maintenance services to perform analysis and condition
29 monitoring of mechanical components and systems. Most common faults in machines are due to rotating
30 components, such as bearings, gears and shafts. The coupling between the rotating part and the frame of
31 the machine is subject to wear, to fatigue effects, poor lubrication or changing environmental conditions.

32 As far as the wear increases the mechanical component breaks, causing unexpected stops of the machine
33 and subsequent economic loss due to lack of production. The accelerometer is a sensor that detects
34 and acquires vibrations of the component it is fixed to, allowing an early detection of the wear before it
35 causes severe damage to the machine, avoiding unexpected stops. Among the so-called Non-Destructive
36 Testing techniques [1], the vibration analysis has a relatively low costs for the sensor and an easy set-up
37 on the machine. All the vibration measurements are normally performed by means of a piezoelectric
38 accelerometer or based on Micro Electro-Mechanical Systems (MEMS) technology. The development of
39 both MEMS and piezoelectric technology leads to better products, resistant to environmental agents, with
40 small dimensions and a great bandwidth. The application of MEMS in many technological products, such
41 as smartphones and gaming application makes these devices extremely low price and very interesting
42 for the vibration monitoring. The introduction of the piezoelectric accelerometer was in the '50s while
43 MEMS technology comes lately, thus a relevant amount of papers on signal processing can be found in
44 technical literature, setting the state of the art on vibration analysis so far [2]. Despite the thousands of
45 papers dealing with the problem of vibration signal processing, there are only few papers which focus on
46 a correct setup of the vibration sensors, even though it is crucial for every accelerometer applications [3].
47 This practical aspect is mainly based on the information retrievable in university courses on vibrations
48 analysis, either on personal experience or to information given by the accelerometer suppliers [4–6]. The
49 supplier' guidelines usually focus on a specific aspects of the accelerometer setup, the mounting between
50 the sensor and the surface of the component. The main solutions available are: screw mounting, stud
51 mounting, magnetic mounting, adhesive mounting and probe mounting. Each method has a specific field
52 of application depending on: the working temperature, the mounting surface conditions, the accessibility
53 to the specific mounting point, etc. A detailed description of all the mounting techniques could be find in
54 classic handbook on shock and vibration [7]. Among other techniques, the adhesive and the screw/stud
55 mounting are the most typical. These mounting techniques result in a rigid connection with high stiffness
56 and wide frequency range response. Compared to screw/stud mounting, structural adhesives are more
57 reliable in the fastening of sensors and accelerometers, since they provide a simple and quick mounting
58 without the need of permanent mechanical processing, such as threaded holes, on the chassis of the
59 machine as stated by Harris [7] as well, while the stud/screw mounting allows a quicker setup on the
60 sensor. In a previous work [8], the authors focuses on the adhesive mounting of accelerometers, assessing
61 experimentally the dynamic response of three different adhesives which cover the most common type of
62 structural adhesive used in on-field applications; namely a two component methylmethacrylate, HBM
63 X60 [9], a cyanoacrylate, Loctite 454, [10] and a modified silane, Terostat 939 [11]. Often it is believed
64 that "soft and rubbery" adhesives, which works above their glass transition temperature, like the modified
65 silane could not be used in this type of application. Secondary objective of the paper is to prove if this
66 sentence, retrievable in literature but with little evidence, is true. By means of an electrodynamic shaker,
67 a design of experiment approach was proposed consisting of three variables in the experimental plan:
68 adhesive type, frequency and amplitude of the vibration signal. The main results proved that the transfer

69 function of the adhesive layer does not distort the signal regardless of the type of adhesive. In this paper,
70 a further step of that research is proposed, investigating the influence of the temperature on dynamics
71 response of the above-mentioned adhesives. The effect of temperature on the adhesives was studied in
72 technical literature [12] and also by other authors [13–16], but scarce information is retrievable on their
73 viscoelastic properties at different temperature when in thin films. The global information is related to
74 their polymeric nature, therefore softer adhesive are more affected by temperature and tend to relax more
75 than the stiffer ones when temperature increase. The aim of the paper is to estimate which is the effect
76 of the adhesive film used to join the parts in terms of vibration monitoring and signal transmission. The
77 adhesives are used to join two aluminium bases, the first one connected with a threaded coupling to an
78 accelerometer and the second one coupled with the head of electromagnetic shaker. The specimens are
79 placed in climatic chamber together with the shaker and the sensors. The description of the experimental
80 procedure and the detailed experimental set up are shown in Section 2.3. The Materials and Method
81 section describes as well the design of experiment approach used. It consists of four variables in the
82 experimental plan: adhesive type, frequency, amplitude of the control signal and temperature of the
83 climatic chamber. The amplitude and the frequency are chosen in order to explore the entire range of the
84 electromagnetic shaker available in the laboratory, while the temperature spans the range available on the
85 climatic chamber (23 °C - 80 °C). A finite element modal analysis, reported in Section 2.4, was carried out
86 in order to estimate numerically the influence of the adhesive layer on the resonant modes of the structures.
87 The results confirm the little influence of the adhesive layer, due to its very low thickness. The Section
88 3.2 shows the detail of the post processing procedure carried out on the experimental data. The signal is
89 post-processed through a LabVIEW environment and four significant output parameters are extracted:
90 the spectral amplitude of the excitation frequency (Spectral Amplitude - SA), the percentage of signal
91 energy stored at the excitation frequency (Stored Energy - SE), and their weight percent over a reference
92 specimen (Spectral Amplitude Ratio - SAR - and Stored Energy Ratio - SER - respectively). These
93 data are elaborated with a statistical software to evaluate which variable affects the system responses
94 and which is the adhesive's effect on the vibration monitoring. The Section 3.3 exploits the ANOVA
95 (Analysis of Variance) technique to estimate which are the most significant effects on the responses
96 by means of half normal plots and variable interactions diagrams. In the conclusions we present some
97 interesting consideration about the adhesive bonding of the accelerometers and some practical hints useful
98 in laboratory and industrial environment are presented.

99 **2 METHODS AND MATERIALS**

100 **2.1 Design of Experimental plan**

101 The Design of Experiments (DoE) method was developed to optimize the experimental tests especially
102 for multiple variables involved in a problem [17]. The same principles can be also stretched to numerical
103 studies [18], treating each numerical analysis with a different set of levels and variables as a *virtual*
104 *experiment* . In the present work the DoE technique was used to assess the effect of the temperature and of

105 the input excitation on the dynamic mechanical response of adhesive mounting accelerometers at different
106 working conditions. Four factors were considered in the analysis, namely:

- 107 1. Adhesive type, G
- 108 2. Excitation amplitude, A
- 109 3. Temperature, T
- 110 4. Excitation frequency, f

111 A previous paper of the authors [8], analyzed the effect of the frequency and the amplitude on different
112 adhesive bonding, although the chosen levels were different. A cross-check of the results with the ones
113 obtained in the previous work, will be still possible.

114 The levels of the excitation frequency have been chosen based on a resonance test on a reference
115 specimen at room temperature. The shaker was excited by a linear sine sweep signal in all the shaker
116 frequency range, i.e. from 0 to 12kHz, with a rate of 1kHz/s. The acquired vibration in time domain is
117 shown in the left part of Fig. 1, revealing the presence of a resonance peak at 7 seconds. The right part of
118 Fig. 1 shows the corresponding frequency spectrum, fixing the resonance at 7485Hz. It is worth noting
119 that the high amplitude at low frequency is not a resonance of the system, but a limit in the performances
120 of the shaker, optimized to work at mid-high frequencies.

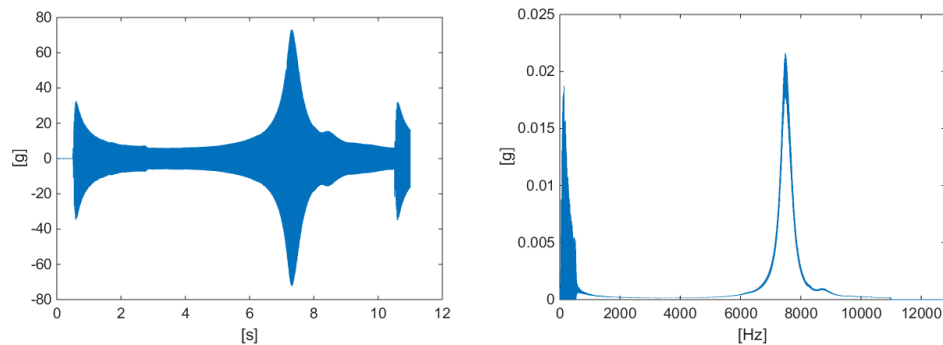


Figure 1. Frequency sweep and resonant peak of the acquisition test rig

121 Based on the sweep test, the three levels of excitation frequency f are chosen viz. 15 Hz, 3500
122 Hz, 10000 Hz in order to span the entire range of the accelerometer [19], taking into account also the
123 non-linear behavior at low frequency. It was decided to consider the low frequency range even though the
124 input signal is not clean for two main reasons. The first reason is that at low frequency we have an higher
125 amount of energy and therefore is interesting to monitor these bandwidth. The second reason is that the
126 desired behaviour of the adhesive should not be dependent on the input signal, no matter how bad or
127 distorted is. The values chosen for the excitation amplitude are expressed as a percentage of the maximum
128 amplitude provided by the shaker, i.e. 50% and 100%. The temperature is the core factor of this analysis,
129 so four levels are chosen to better highlight its influence in the tests: 23°C (room temperature), 40°C,

130 60°C, 80°C. We decided not to exceed 80°C since it is practical limit for many rotating machineries
131 driven by electrical motors. Each specimen was stored in the climatic chamber for a proper time before
132 the test, in order to heating up the aluminum specimen checking the surface temperature by means of a
133 infrared thermometer. The adhesive type are the same four used in [8]: G1 is the commercial superglue
134 (Loctite 454), the G2 is an elastic adhesive modified silane (Terostat 939), both produced by Henkel
135 Adhesive, Cerano (NO), Italy. The G3 is a very stiff two components methylmethacrialte adhesive (HBM
136 X60), produced by HBM, Milan, Italy and G4 is a reference configuration in which there is no adhesive
137 but continuum material. A Dynamic Mechanical Analysis (DMA) on the selected adhesives would have
138 been useful, but in literature we could not trace precise information about the viscoelastic behaviour of
139 the adhesives chosen. Moreover the adhesive behaviour in bulk form and in thin film is pretty different
140 [20–23] so the eventual information given by a DMA in bulk are not immediately applicable to thin
141 adhesive layers. Qualitatively the adhesives have very different viscoelastic behaviour, as retrievable
142 on the basis of the chemistry and on the datasheets of the polymers involved [12, 16, 24]. The stiffer
143 adhesives, which works below the glass transition temperature which is 137°C for G1 see [10] and about
144 150°C for G3, see [9] have limited viscous effect, while the softer one (G2) is quite viscoelastic, since it
145 works in its rubbery state at room temperature [11]. A summary of the variable levels is reported in Table
146 1. Each specimen is made by two cylindrical aluminium blocks, connected with a thin layer of adhesive,
147 the lower one is screwed to the shaker, the upper one has a threaded connection for the accelerometer. In
148 the reference configuration (level 4 of "adhesive type" variable in Tab. 1), there is no adhesive between
149 the two blocks but a unique aluminum cylinder with double mass of a single block, in order to keep the
150 same nominal natural frequency. The authors decided to set the adhesive layer thickness at a constant
151 value of 0.05mm and then to exclude it from the experimental plan even though it is important in the
152 adhesive stiffness and strength [12–17]. The adhesive thickness is typically an uncontrolled parameter in
153 a practical application of a bonded accelerometer and, the thickness is controlled by the surface roughness
154 only. The description of the deposition of the adhesive layer and the curing process is reported in Section
155 2.3.

Variables	Level 1	Level 2	Level 3	Level 4
Temperature, T	23 °C	40 °C	60 °C	80 °C
Frequency, f	15 Hz	3500 Hz	10000 Hz	
Amplitude, A	50%	100%		
Adhesive type, G	Loctite 454	Terostat 939	HBM X-60	None (solid)

Table 1. Levels of the variables considered in the DOE

156 A full factorial plan is adopted, with two replicates for each experimental plan. This approach is
157 combined with a blocking procedure to take into account the different bonding of the adherends. The
158 blocking procedure is a useful tool, used in the DoE approach, in order to avoid any influence of the
159 experimental set up or the operator, as described in [17, 18, 25]. Four different temperatures, three
160 frequencies, two amplitudes, four adhesives and two replicates lead to a total amount of 144 experiments

161 on the bonded configuration, which can be used to estimate the influence of the primary variables and the
 162 interactions. Further 48 additional experiments on the reference configuration were carried out, leading
 163 to a total of 192 experiments. We exploited the software Design Expert in order to build the set of
 164 experimental test to be carried out and to randomize the order of the experiments. The software was also
 165 used to post process some of the results using mainly an analysis of variance technique (ANOVA).

166 2.2 System response

167 The statistical influence of the variables is evaluated in terms of four system responses. The shaker
 168 excitation is a sinusoidal wave at a given frequency, therefore the amplitude of the corresponding spectral
 169 component is the main output choice. The two main of the outputs of the experiments are:

- 170 • Spectral amplitude at excitation frequency (SA)
- 171 • Percentage of signal energy stored at excitation frequency (SE)

172 The SA is obtained by applying the Fast Fourier Transform to the vibratory signal, considering the
 173 amplitude of the measured signal at the excitation frequency, the SE is the energy of the vibratory signal
 174 at the excitation frequency divided by the total energy of the system.

175 Other two outputs are computed dividing the values of the experimental points by the value of the
 176 reference configuration (on average). The block with double mass and no adhesive is taken as reference
 177 configuration. These outputs are not dependent on the system configuration and allow the adhesive effect
 178 to be compared more efficiently. The two additional parameters are:

- 179 • $SAR = SA/SA_{no_adhesive}$ Spectral amplitude ratio (SAR)
- 180 • $SER = SE/SE_{no_adhesive}$ Stored energy ratio (SER)

181 The four parameters (SA, SE, SAR, SER) were firstly proposed in [8].

182 2.3 Experimental set-up

183 The experimental set-up consists in the test specimens, a climatic chamber, a small electrodynamic shaker,
 184 a monoaxial accelerometer, a data acquisition board and a function generator. Table 2 summarizes the
 185 model and the characteristics of the components.

Component	Model	Specifications
Climatic chamber	homebuilt	2x600W fan heater - PT100 temperature sensor, Ascon hysteresis controller, precision 23 °C
Shaker	ModalShop K2004E01	20 N peak sine force, frequency up to 11 kHz
Accelerometer	PCB 353B18	Monoaxial, freq. range 1-10 kHz ($\pm 5\%$), 10 mV/g
DAQ	NI USB-9162 + NI-9233	50 kS/s per channel, 24-Bit IEPE
Function generator	Rigol DG1022	2 channels, 20 MHz waveform generator

Table 2. Specifications of the components used in the experiment.

186 All the specimen blocks are built from a single aluminum bar, with a circular cross section of 10 mm
 187 of diameter. Each block is 20mm high, except the reference block that has a double height 40mm, being

188 negligible the adhesive weight. The size of the blocks is chosen to ensure space for the threaded hole,
189 but still keeping enough mass in order to have a stiff specimen. All the blocks have been threaded to be
190 coupled with the shaker head and the accelerometer by means of an adaptor. The blocks were bonded
191 using a jig to maintain alignment between the upper and lower one and a small dead weight (0.1 kg)
192 was used to apply a sufficient pressure to the entire adhesive layer. The adhesive fillet is removed with
193 a cutter immediately after the applications, in order to avoid any extra mass and due to the very fast
194 curing (few seconds) of the Loctite 454 and XBM X60. In order to achieve complete polymerization we
195 kept all the joints at room temperature for 48h, to ensure a proper curing of all the three adhesives. The
196 estimated nominal thickness is 0.05mm. The eight specimens (4 adhesive levels and 2 replications), the
197 accelerometer and the acquisition board are shown in Fig. 2. The shaker is provided with an embedded
198 amplifier, open-chain controlled with 0-1 VRMS signal supplied by a Rigol function generator. The
199 shaker is equipped with an amplitude gain which can be selected by the user, but in this experiment
200 we decided to keep it constant for all the tests. The accelerometer is acquired by means of a NI-9233
201 board which is specifically designed for IEPE devices. The shaker is fixed to the ground of the climatic
202 chamber, while the shaker body is connected to its fixed frame by vises. In each test the head of shaker
203 moves harmonically with characteristics listed in Table 2. The amplitude is not measured in absolute
204 “g” value, but it is expressed by a percentage of the maximum control voltage, i.e. with a V_{peak} value
205 of 1V for the 100% of amplitude and 0.5V for the 50% amplitude. The sampling frequency is 50 kHz
206 and the acquisition time is 3 seconds. The acquisition system waits two seconds before starting to avoid
207 acquisition of undesirable transient effects of the shaker. The climatic chamber is home built, made in
208 PVC insulating panels (12mm thick) with two fan heater (600W each) controlled by an Ascon controller.
209 The controller ensures the desired temperature by means of a PT100 thermocouple and implements
210 a threshold control with a mean error of 0.5 °C. The fans, integrated in the heater ensure an uniform
211 temperature distribution in the climatic chamber. Figure 3 shows the final setup of the shaker in the
212 climatic chamber.

213

214 **2.4 Finite Element Model**

215 This section describes a preliminary analysis of the system carried out by means of a finite element modal
216 analysis. The aim of the parametric analyses is to assess the theoretical influence of the adhesive layer on
217 the natural frequencies of the system considered. Four different analyses were carried out: three different
218 adhesives and the reference configuration are modelled. The finite element modal analyses are carried
219 out by using Abaqus 6.141 FEA solver. The model is composed by two aluminum blocks with the exact
220 dimensions of the specimen described in the previous sections, bonded by a 0.05mm thick adhesive layer.
221 The mesh continuity guarantees that no contact elements disturb the transition between different materials.
222 The model used for the reference configuration shares the same mesh with the other three bonded models.
223 The accelerometer weight is considered and the threaded connection of the accelerometer is modelled as a

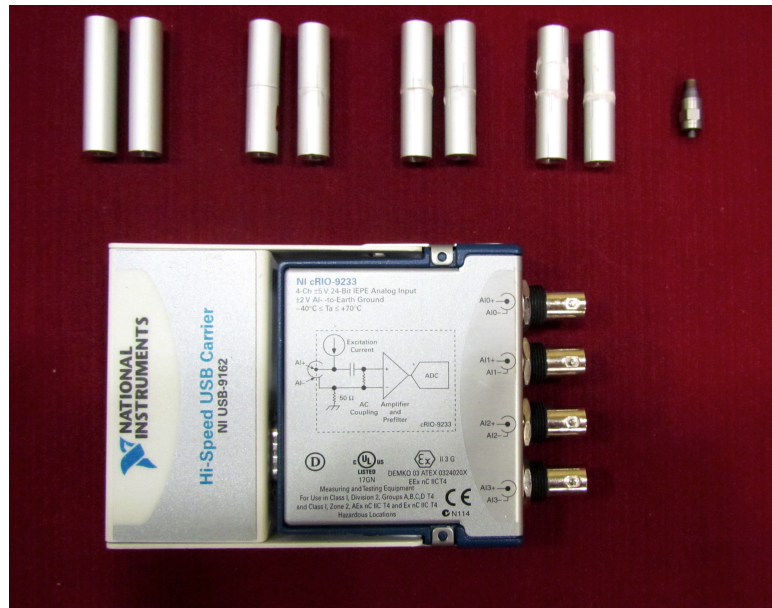


Figure 2. Experimental specimens, accelerometer and acquisition board

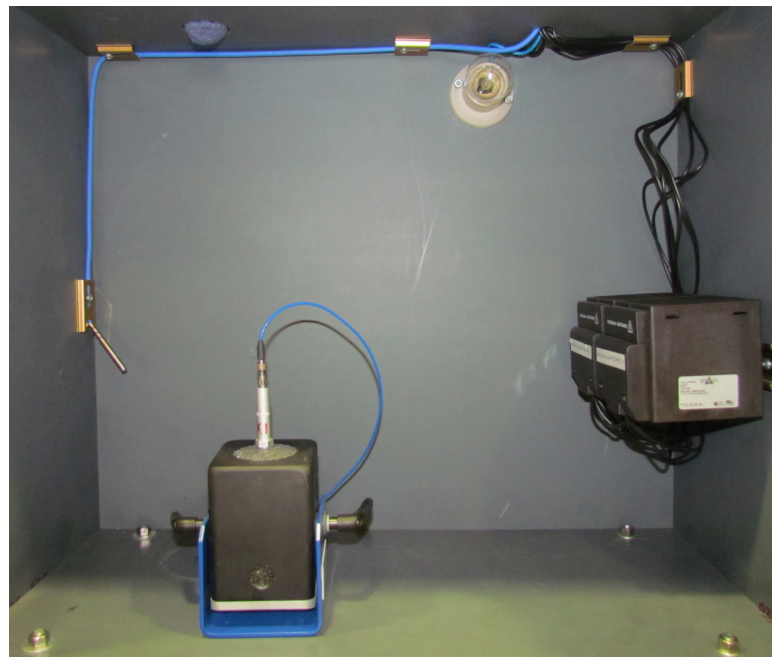


Figure 3. Experimental test rig with climatic chamber and mini shaker

224 perfect contact in each case. The model is implemented with linear hexahedral elements with standard
 225 formulation, 1223470 nodes and almost 3.5 million d.o.f. The need of having so much elements is driven
 226 by the very low thickness of the adhesive. In order to have undistorted elements in the adhesive layer,
 227 which is crucial for the analyses, we had to force a very refined mesh size in that region. This is a very
 228 common problem, as reported by many authors [26–28] The elastic moduli of the three adhesives are
 229 taken by the technical data sheets in literature and span from 100 MPa for the Terostat 939 to 800 MPa

230 for the Loctite 454 and 4000 MPa for the X60 - HBM adhesive. We considered room temperature for all
231 the adhesives, leaving the evaluation of the temperature effect to the experimental part. The boundary
232 condition applied is to prescribe at 0mm the nodal displacement of the basis, as shown using orange
233 triangles in Figure 4 in order to be consistent with the experimental tests. The frequency domain is limited
234 to 20kHz, in order to save computational time and do not exceed the experimental limit given by the
235 mini-shaker. As output we can compare the natural frequencies of the bonded models with the frequency
236 obtained using the reference and with the experimental results.

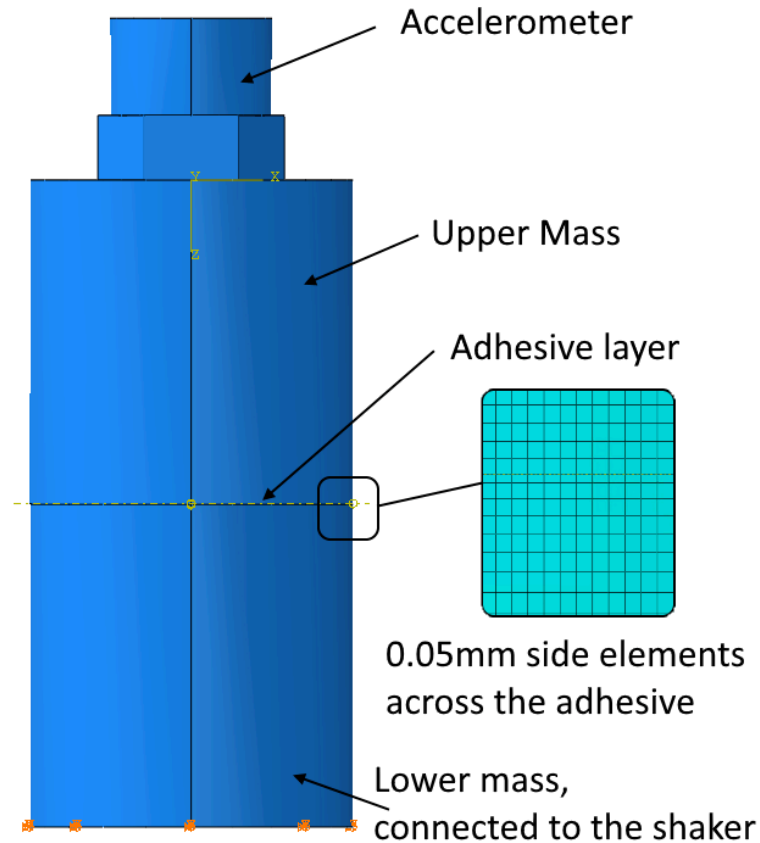


Figure 4. Boundary conditions applied to the FE model and magnification of the mesh of the adhesive layer

237 **3 RESULTS AND DISCUSSION**

238 **3.1 Finite element model results**

239 This section describes the finite element model results, showing the effect of the three materials and
240 comparing the natural frequencies with the experimental results. The finite element model results can
241 be qualitatively expressed by the modal form of the system and their natural frequencies. The modal
242 forms of the systems are the same for all the four models and are reported, just for the Loctite 454 case, in
243 Figure 5. It is important to note that with adopted linear perturbation analysis, the value of the magnitude

244 is not significant. The most important information is given by the frequencies of these three modal forms.
 245 We report in Table 3 the natural frequencies obtained in the four cases. The modal analysis confirms that
 246 the peak at nearly 7kHz is due to a natural resonance of the system, as shown in 1 and it is important to
 247 note that this peak is almost not affected by the presence of the adhesive. The softer one and the reference
 248 configuration differ only of less than 5%. This first result shows that the presence of the adhesive, thanks
 249 to its very low thickness, do not modifies substantially the harmonic behaviour of the system, and therefore
 250 confirms the previous authors' finding [8]: choosing a general adhesive rather than a specific one does not
 251 affect the system behaviour. The experimental test will show whether or not the temperature will change
 252 this kind of behaviour.

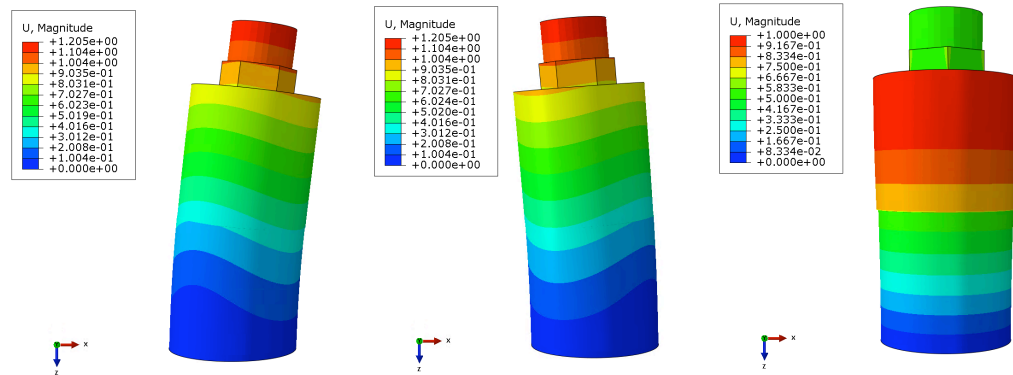


Figure 5. Modal forms of the system. From left to right, bending on first plane, bending on second plane, torsion along the axis

Adhesive type	E (MPa)	ni	rho (kg/m3)	1st (Hz)	2nd (Hz)	3rd (Hz)
Terostat 939	100	0.45	1500	6736.5	6736.6	17712
Loctite 454	800	0.3	1100	6738.3	6738.4	18262
HBM X60	4000	0.3	800	6889.7	6889.9	19046
None (reference)	-	-	-	6926.8	6926.9	19234

Table 3. Natural frequencies of the finite element model.

253 3.2 Post-processing of the experimental data

254 The post processing of the vibration data was done in National Instruments' LabVIEW 2016 environment.
 255 In order to avoid transient effect on the acquisition, the tails of the vibration signal are removed, i.e. 0.5
 256 seconds at the beginning and at the end of the signal are removed from the 3 second of acquired data. The
 257 resulting 0.5 Hz of spectrum resolution allows to clearly match the excitation frequencies. The system
 258 response if computed by means of the power spectrum of the vibration data, as reported in equation 1.

$$PS(f) = \frac{FFT^*(\bar{x}) \cdot FFT(\bar{x})}{n^2} \quad (1)$$

259 where $FFT(\bar{x})$ is the fast Fourier transform (FFT) of vibration data, while the FFT^* denotes the
260 complex conjugate and n is the length of samples array. In an ideal condition, the sine input of the shaker
261 — measured by the accelerometer — returns a single peak as output in the frequency domain, at the
262 excitation frequency f_{ex} . An interesting comparison among different adhesive type is made on two scalar
263 output parameters (despite connected):

- 264 • The amplitude of the power spectrum at the excitation frequency (SA).
- 265 • The ratio between the amplitude of the spectrum at the input frequency and the total energy of the
266 acquired vibration signal (SE).

267 The choice of these parameters follows a simple reasoning: SA is what is usually measured in
268 experimental activity, i.e., it is a measure of absolute value depending of the energy at input source, while
269 SE returns the quality of the acquired signal independently of the energy of input source. A further
270 consideration is given by The Parseval's theorem, regarding the choice of the power spectrum instead of a
271 simple spectrum. In fact, the theorem states that the total energy contained in a time-domain waveform is
272 equal to the total energy of the waveform' spectrum. The equality is reported in Equation 2.

$$\int_{-\infty}^{+\infty} |x(t)|^2 dt = \int_{-\infty}^{+\infty} |X(f)|^2 df \quad (2)$$

273 It follows that the total energy of the signal can be computed as a simple sum of power spectrum
274 components.

275 Two other outputs are computed dividing the values of the experimental points by the value of the
276 reference configuration (on average), as mentioned in Section 2.2. The two parameters are named SAR
277 and SER since they are derived from the SA and SE values respectively.

278 **3.3 Statistical analysis of the results: Analysis of Variance**

279 There are many statistical methodologies to tackle the analysis of multivariate problems [29]. Among
280 these we adopted the Design of Experiment (DoE) procedure, a powerful statistical technique based on
281 the analysis of variance (ANOVA) that can be conveniently applied to these classes of problems. ANOVA
282 is based on the variance calculation (standard deviation) of a response considering the single variable and
283 also the global variance of the responses. The ratio between these two quantities is called the F-value
284 [29]. When we consider a random process this F-value equals one, meaning that the variable under
285 analysis has no tangible effect on the selected response, since it behaves the same way as the experimental
286 noise for practical test or numerical error for parametric simulation. On the contrary a larger F-value
287 means can be associated to a variable that influences the process. Among the several approaches typically
288 used to represent the results graphically one of the most popular is the normal plot. It is used mainly
289 to demonstrate which are the main consequences of the variables on the system response, estimating
290 whether a certain set of data follows a Gaussian distribution or not. When the data are approximately

291 a straight line the response is statistically "normal" i.e. follows a stochastic law. When the selected
292 variable strongly affects the system response its effect, reported in the normal plot, will then fall outside
293 the normal distribution line. This line, also called errors line is built up thanks to the replicates of the
294 experimental tests which have the variability typical of the experiment considered and their effect has a
295 normal distribution. The replicates of the experiments are therefore important because they are used to
296 build the error line because they are ruled by a stochastic law by definition. The greater the deviation of
297 the point from the normal line the larger the confidence interval (i.e. the probability that the variables are
298 significant is higher). In this paper we adopted the half normal plot, which behaves in the same way as the
299 normal plot, but considers only the absolute significance of the variables and not their sign.

300 **3.3.1 Half-normal plot of the response**

301 Figure 6 shows the half-normal probability plots from an ANOVA following [17]. The analysis was
302 performed on two outputs of the problem (system response) described in the previous subsection. Figure
303 6 shows the SA, Figure 7 the SE. In Figure 6 and 7 on the X-axis is represented the standardized effect
304 linked to each factor considered. The higher the standardized effect, the greater the influence of the
305 variable on the response. The Y-axis represents the half-normal probability associated with each effect.
306 The greater the Y value the higher the probability that the effect has an influence on the problem. The
307 solid line is the error line, which is obtained by interpolation of the replicates of the tests, represented
308 by triangles, and also the high order interactions of the variables, represented by the squares, which do
309 not play any role on the system response. The points that fall off the error line represent the factors that
310 mainly affect each response. Figure 6 and 7 show that the frequency and the amplitude have the strongest
311 influence both on SA and SE. The effect of the frequency is the most relevant both for SA and SE. It
312 must be noted that we applied a transformation to the selected variables, in order to normalize the data.
313 This linearization, called Box-Cox transformation, is strongly recommended [18] when there is the need
314 of dealing with experimental set of data by means of ANOVA technique, which gives better prediction
315 for linear problems. In Figure 6 the effect of the variables are reported applying an inverse square root
316 transformation and in figure 7 we have SE raised to the power of 2.2. The amplitude is relevant in both
317 cases, while the interaction between frequency and amplitude is more important for SE than SA. The half
318 normal plots of the SAR and SER are reported in Figure 8 and Figure 9 respectively. These Figures show
319 that dividing SA and SE by the reference configuration causes two different behaviors.

320 The SAR chart Figure 8 shows a strong dependence on the temperature (D) and on the interaction
321 between frequency (A) and temperature (AD). The amplitude of the signal disappears when compared
322 with Figure 6. The SER chart Figure 9 shows a more complex situation. In this case the amplitude and
323 the frequency are important as it happens for the SE as shown in Figure 7 and in addition the temperature
324 plays a secondary but still relevant role.

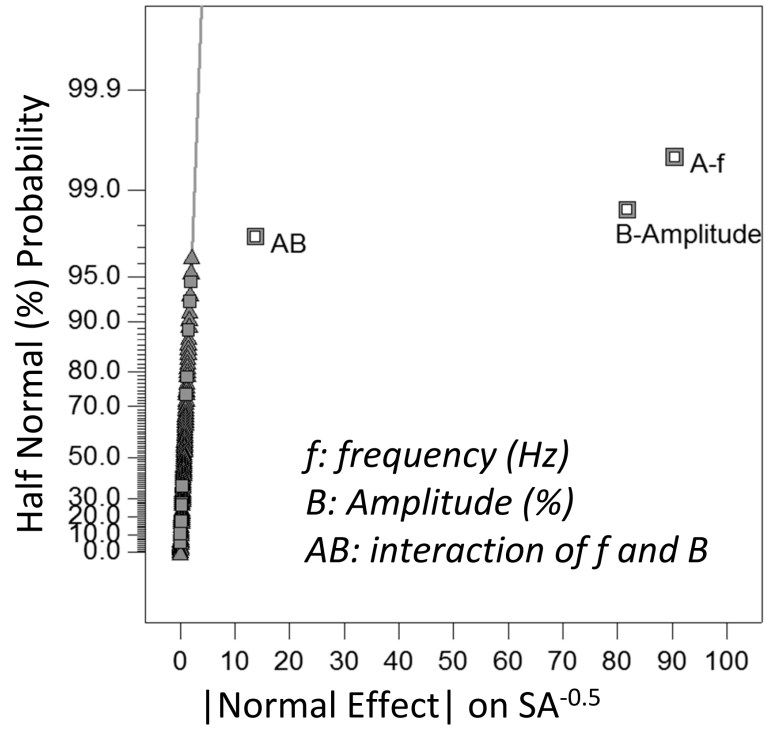


Figure 6. Half normal plot of the SA, with an inverse square root transformation applied

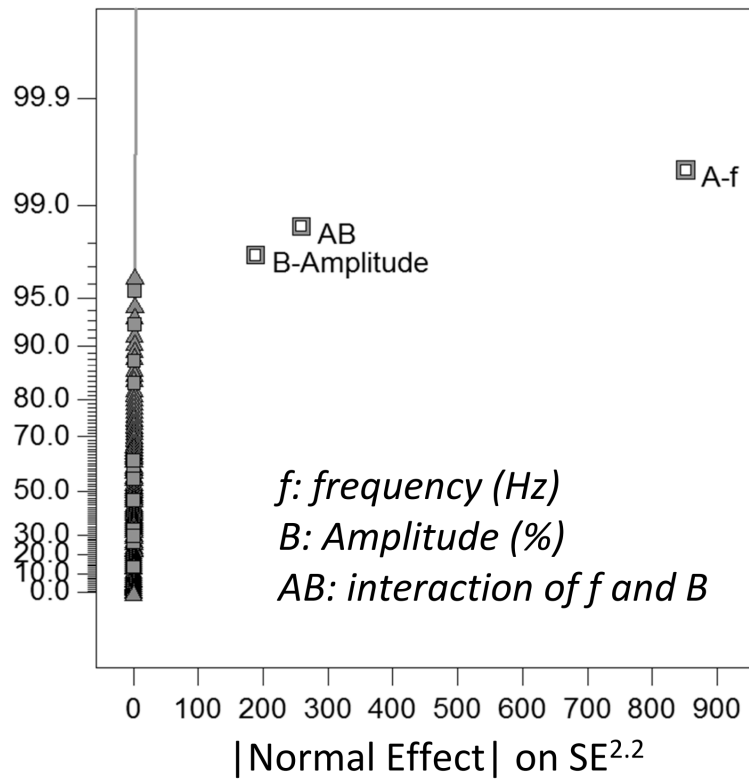


Figure 7. Half normal plot of the SE, with a power law transformation applied

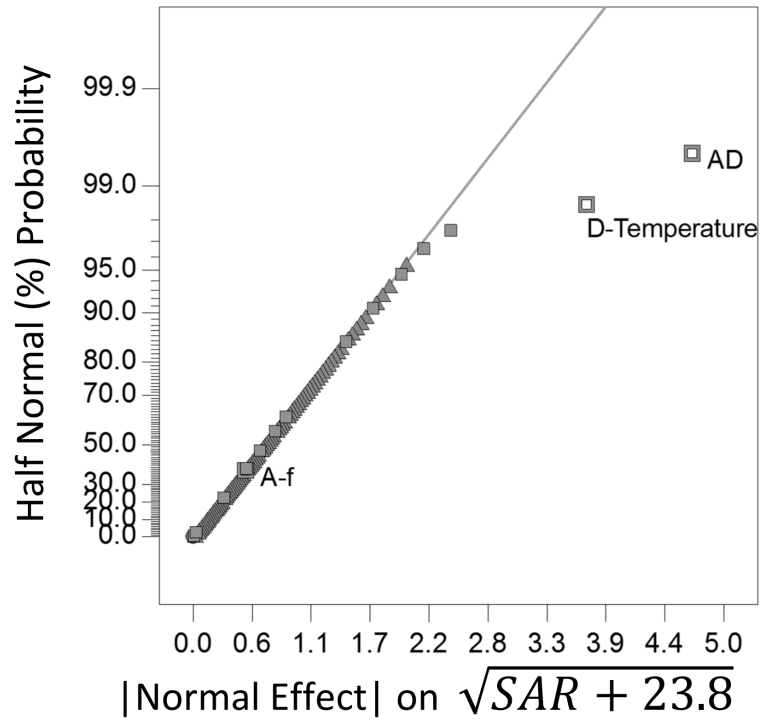


Figure 8. Half normal plot of the SAR

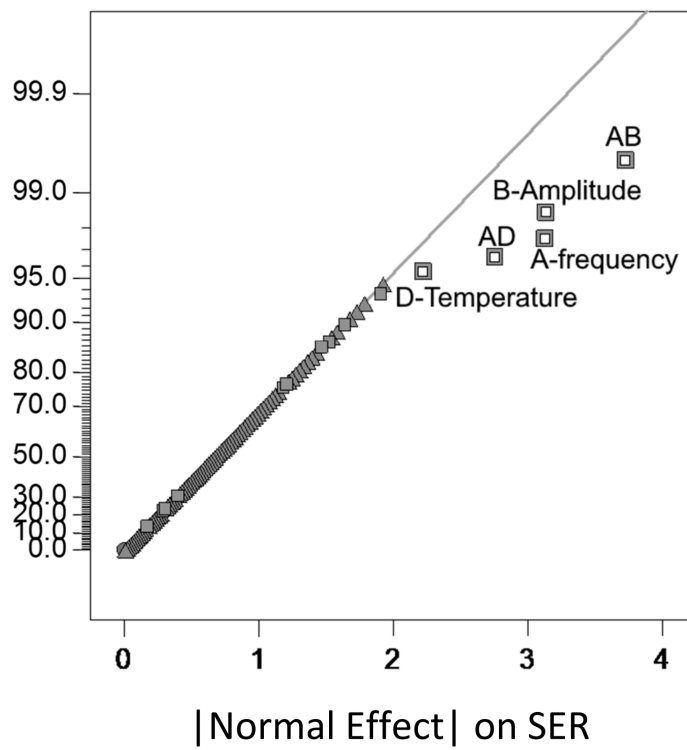


Figure 9. Half normal plot of the SER

325 **3.3.2 Variable interactions and relevance**

326 Two main comments can be drawn by the graphs in Figure 6, 7, 8 and 9. The first one is that the adhesive
327 type is not relevant compared with the other variables. This is the most important finding of this research
328 since it tells us that no matter the adhesive stiffness and the adhesive strength the bond between the
329 excitation base and the accelerometer base is enough to transmit a correct signal. Therefore we can choose
330 the most suitable adhesive according to other considerations such as cost, simplicity, availability and ease of
331 application. The second important consideration is that the temperature somehow is relevant for SAR and
332 SER. This means that it could be important to monitor the temperature as well as the vibration if we want
333 to be sure of taking into account all the possible sources of variations. In order to show the direct influence
334 on the four system responses of the selected variables we can take advantage of the following graphs.
335 Figure 10 shows that the system has larger values of SA with increasing frequency and amplitude. These
336 two variables present an interaction clearly visible due to the divergence of the two interpolating lines.
337 The points in the graph represent the experimental results obtained and it is visible the good repeatability
338 and the scarce significance of the other variables. Figure 11 shows a completely different situation. The
339 main effect on SE is at the lower frequency, where we can see a difference due to the amplitude. It must
340 be noted that the mini-shaker at 15 Hz shows some issues, as reported in Figure 1. We did not expect a
341 behavior like that, therefore we are investigating on this problem, to see if the behavior is due to the noise
342 at low frequency. The SE parameter describes how many portions of the system's energy is transmitted at
343 a given frequency with respect to the total one. Probably, the non-linearities at low frequencies make the
344 SE response sensible to the amplitude. It is worth noting that anyway no sign of a significant influence
345 of the adhesive nor the temperature can be found as well. Disregarding the data at 15 Hz would lead to
346 a substantial independence of SE on the other variables. Figure 12 shows the effect of the temperature
347 and of the frequency on the SAR. In this case, in order to show the actual values we did not apply the
348 Box-Cox transformation as we did in Figure 8. The figure 12 shows three curves, as a function of the test
349 temperature. The red squares represent the 15 Hz tests, the green triangles depict the 3500 Hz tests and the
350 blue dots the 7000 Hz tests. The adhesive and the amplitude have no effect, but they appear only as the
351 error bars in the three curves. As for the SE the SER results, shown in Figure 13 is affected by the
352 results at 15 Hz. We can easily spot a difference in the two amplitudes and frequencies as a function of
353 the temperature, but it is much more evident at 15 Hz rather than at the other frequencies. It is useful to
354 highlight that, even though there is some noise at 15 Hz, the experimental tests show a clear absence of the
355 adhesive in each statistical analysis performed. This is the main outcome the authors wanted to find out
356 and therefore the conclusion is that the bonding does not change the vibratory signal from the source to the
357 sensor, even considering soft adhesive such as the Terostat 939 or when the test temperature increases up
358 to 80 °C.

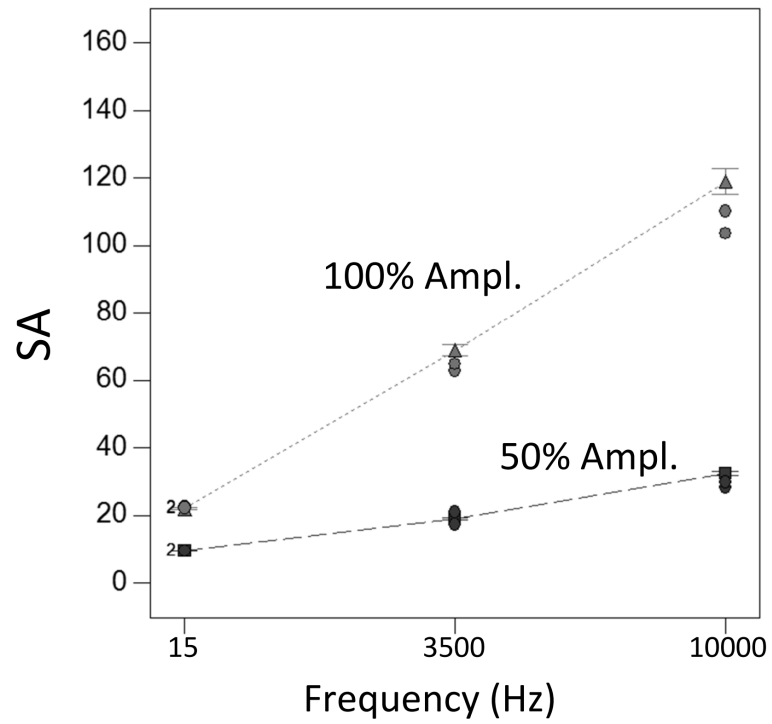


Figure 10. Effect of the main variables on SA

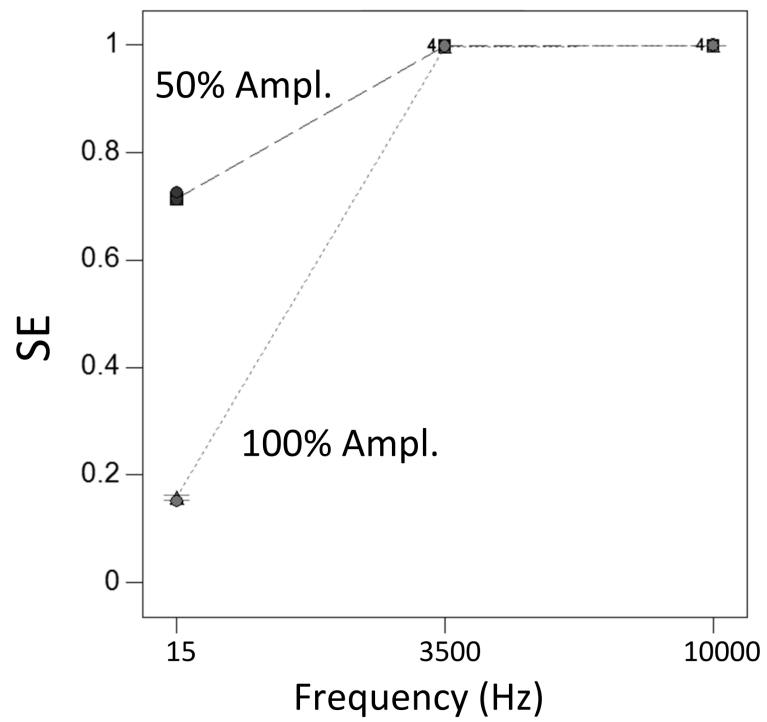


Figure 11. Effect of the main variables on SE

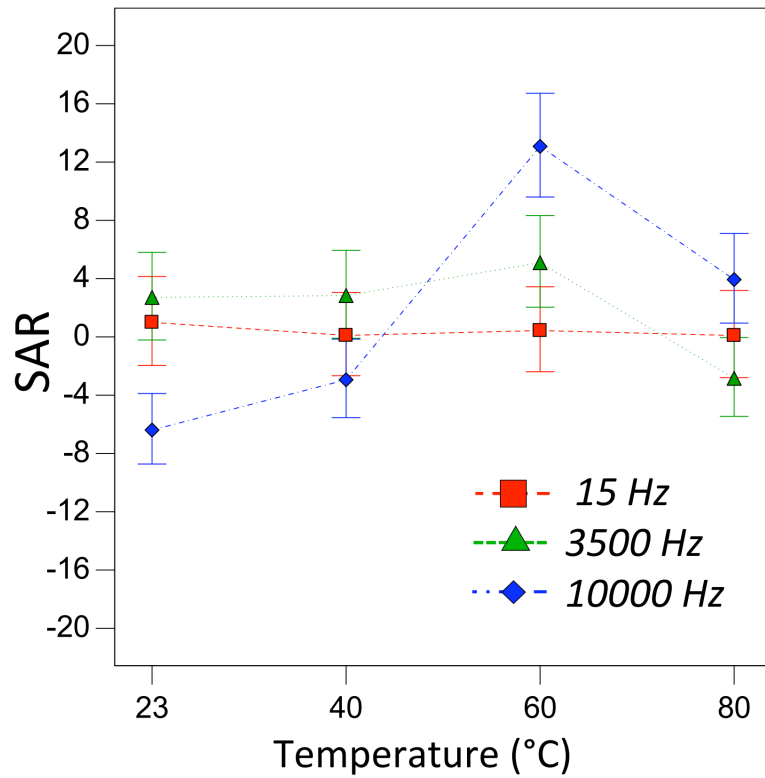


Figure 12. Effect of the main variables on SAR

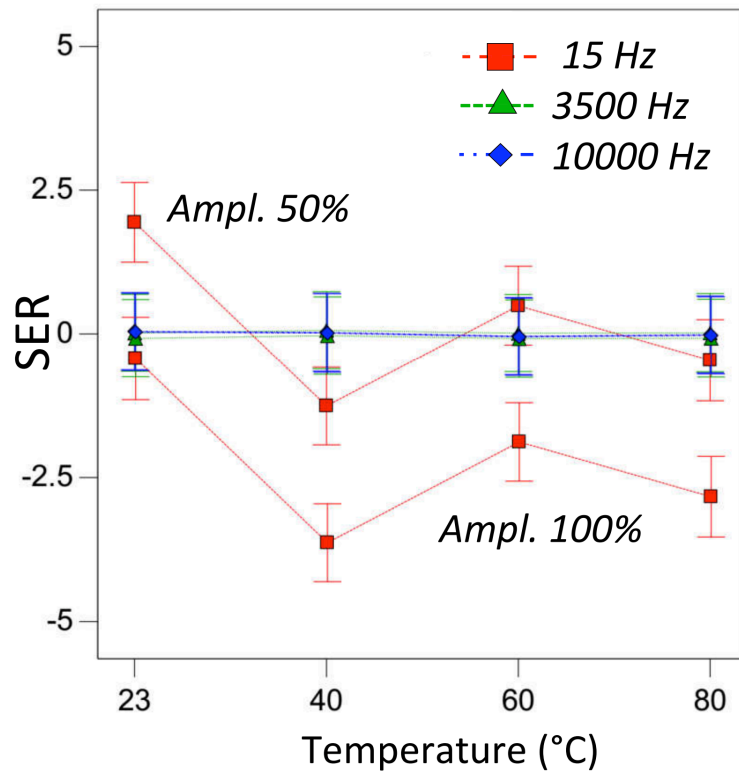


Figure 13. Effect of the main variables on SER

4 CONCLUSION

This paper focuses on the effect of temperature on the frequency response function (FRF) of three different structural adhesives, namely a stiff two component methylmethacrylate (HBM X60), a soft modified silane (Terostat 939) and a cyanoacrylate superglue (Loctite 454). The methylmethacrylate is commonly used in strain gauge application and accelerometers setup in on-field environments due to its stiffness. The cyanoacrylate is the most used in accelerometers setup for diagnostics purposes in laboratory due to its fast polymerization time. The silane is a general purpose adhesive chosen for its different structural characteristics compared to the other two. They have been used to joint two aluminium cylinders, one connected to an accelerometer and the other to the head of an electromagnetic shaker. A reference additional experiment has been carried on a double-weight aluminium base, simply obtained using a continuum block of double length without any adhesive. The experimental setup is placed inside a climatic chamber providing a selectable temperature up to 80 °C. The shaker provides a sinusoidal vibration in terms of acceleration at different combinations of frequency and amplitude, as summarised in Table 1. A monoaxial accelerometer is used to acquire the feedback vibration signal which has been processed to compute four different parameters assessing the dynamic response of the structure. The output parameters are all computed through the power spectrum of the vibratory signal. They are: SA, i.e the amplitude of the spectrum at the shaker excitation frequency, SE, i.e the ratio between SA and the total energy of the signal, SAR and SER i.e. the values of SA and SE for a given adhesive compared to the corresponding values in the reference condition. The numerical model developed shows that the presence or absence of the adhesive layer does not modify or disturb the natural frequency of the system.

A design of experiments (DOE) approach was used to extract the main conclusions which are summarized as follows:

- Frequency and amplitude have the strongest influence on both SA and SE
- The temperature has a strong influence on SAR
- The SER is influenced by the frequency, the amplitude and the temperature
- The amplitude and temperature have an evident effect on the SA
- No sign of a significant influence of the adhesive nor the temperature can be found on SE, SAR and SER

Above them two results can be used as design guidelines: no matter the adhesive stiffness and the adhesive strength the bond between the excitation base and the accelerometer base is enough to transmit a correct signal. Therefore the most suitable adhesive can be chosen according to other considerations such as cost, simplicity, availability and ease of application. The temperature somehow is relevant for SAR and SER. This means that it could be important to monitor the temperature as well as the vibration if we want to be sure of taking into account all the possible sources of variations.

COMPLIANCE WITH ETHICAL STANDARD

Conflict of Interest: The authors declare that they have no conflict of interest.

REFERENCES

- [1] C. Hellier, *Handbook of Nondestructive Evaluation, Second Edition*. 2012.
- [2] C. Aszkler, “Acceleration, Shock and Vibration Sensors,” in *Sensor Technology Handbook*, pp. 137–159, 2005.
- [3] S. Bowers, K. Piety, and R. Piety, “Real World Mounting of Accelerometers for Machinery Monitoring,” *Sound and Vibration*, vol. 25, no. 2, pp. 14–23, 1991.
- [4] Dytran, “Dytran Accelerometer Mounting Considerations,” 2015.
- [5] PCB, “Introduction to Piezoelectric Accelerometers,” 2015.
- [6] MMF, “Metra Mess und Frequenztechnik in Radebeul,” 2015.
- [7] C. Harris, A. Piersol, and T. Paez, *Harris’ shock and vibration handbook*. 2002.
- [8] M. Cocconcelli and A. Spaggiari, “Mounting of accelerometers with structural adhesives: experimental characterization of the dynamic response,” *The Journal of Adhesion*, vol. 8464, no. March, pp. 1–14, 2015.
- [9] Hbm X60 Datasheet, “Instructions for use Superglue X 60,” 2013.
- [10] Henkel, “Loctite 454 Technical Datasheet,” 2012.
- [11] Henkel, “Terostat 737 Technical Datasheet,” 2015.
- [12] R. D. Adams and N. A. Peppiatt, “Stress analysis of adhesive-bonded lap joints,” *The Journal of Strain Analysis for Engineering Design*, vol. 9, no. 3, pp. 185–196, 1974.
- [13] E. Koricho, E. Verna, G. Belingardi, B. Martorana, and V. Brunella, “Parametric study of hot-melt adhesive under accelerated ageing for automotive applications,” *International Journal of Adhesion and Adhesives*, vol. 68, pp. 169–181, 2016.
- [14] Z. Jia, D. Hui, G. Yuan, J. Lair, K.-t. Lau, and F. Xu, “Mechanical properties of an epoxy-based adhesive under high strain rate loadings at low temperature environment,” *Composites Part B: Engineering*, vol. 105, pp. 132–137, 2016.
- [15] A. K. Kadiyala and J. Bijwe, “Investigations on performance and failure mechanisms of high temperature thermoplastic polymers as adhesives,” *International Journal of Adhesion and Adhesives*, vol. 70, pp. 90–101, 2016.
- [16] L. F. da Silva and R. Adams, “Adhesive joints at high and low temperatures using similar and dissimilar adherends and dual adhesives,” *International Journal of Adhesion and Adhesives*, vol. 27, pp. 216–226, 4 2007.

- 425 [17] D. C. Montgomery, "Design and Analysis of Experiments," *Design and Analysis of Experiments*,
426 p. John Wiley and Sons, 2004.
- 427 [18] R. Mead, *The Design of Experiments: Statistical Principles for Practical Applications*. Cambridge
428 University Press, 1990.
- 429 [19] PCB, "Technical Datasheet PCB Accelerometer 353B18_N," 2017.
- 430 [20] D. Castagnetti, A. Spaggiari, and E. Dragoni, "Robust Shape Optimization of Tubular Butt Joints
431 for Characterizing Thin Adhesive Layers under Uniform Normal and Shear Stresses," *Journal of*
432 *Adhesion Science and Technology*, vol. 24, pp. 1959–1976, 1 2010.
- 433 [21] J. J. Cognard, R. Créac'hcadec, L. Sohier, P. Davies, R. Creac'Hcadec, L. Sohier, R. Creach-
434 cadec, P. Davies, L. Sohier, and P. Davies, "Analysis of the nonlinear behavior of adhesives in
435 bonded assemblies—Comparison of TAST and Arcan tests," *International Journal of Adhesion and*
436 *Adhesives*, vol. 28, pp. 393–404, 12 2008.
- 437 [22] L. Sohier and P. Davies, "Analysis of the nonlinear behavior of adhesives in bonded assemblies —
438 Comparison of TAST and Arcan tests," *International Journal of Adhesion and Adhesives*, vol. 28,
439 pp. 393– 404, 2008.
- 440 [23] A. Spaggiari, E. Dragoni, and H. F. Brinson, "Measuring the shear strength of structural adhesives
441 with bonded beams under antisymmetric bending," *International Journal of Adhesion and Adhesives*,
442 vol. 67, pp. 112–120, 2016.
- 443 [24] K. S. Kwan, *The Role of Penetrant Structure on the Transport and Mechanical Properties of a*
444 *Thermoset Adhesive*. PhD thesis, Blacksbrurg, VirginiaTech, 8 1998.
- 445 [25] M. J. Anderson and P. J. Whitcomb, *DOE Simplified: Practical Tools for Effective Experimentation*,
446 *Third Edition*. Productivity Press, 3rd ed., 2015.
- 447 [26] D. Castagnetti, A. Spaggiari, and E. Dragoni, "Efficient finite element modeling of the static collapse
448 of complex bonded structures," *International Conference on CRACK PATHS (CP 2009)*, 2009.
- 449 [27] D. Castagnetti, E. Dragoni, and A. Spaggiari, "Failure analysis of bonded T-peel joints: Efficient mod-
450 elling by standard finite elements with experimental validation," *International Journal of Adhesion*
451 *and Adhesives*, vol. 30, no. 5, pp. 306–312, 2010.
- 452 [28] M. Tsai and J. Morton, "An evaluation of analytical and numerical solutions to the single-lap joint,"
453 *International Journal of Solids and Structures*, vol. 31, pp. 2537–2563, 9 1994.
- 454 [29] P. Ito, "7 Robustness of ANOVA and MANOVA test procedures," *Handbook of Statistics*, vol. 1,
455 pp. 199–236, 1980.